Original Article

Simultaneous Application of High-Intensity Focused Electromagnetic and Synchronized Radiofrequency for Fat Disruption: Histological and Electron Microscopy Porcine Model Study

Robert A. Weiss, MD, FAAD,* Jan Bernardy, PhD,† and Frantisek Tichy, CSc‡

BACKGROUND Radiofrequency (RF) and high-intensity focused electromagnetic (HIFEM) technologies are used for noninvasive body shaping as standalone modalities.

OBJECTIVE To examine the effects of novel synchronized RF and HIFEM on subcutaneous adipose tissue in a porcine animal model.

MATERIALS AND METHODS Seven large white pigs aged 6 months received 3 abdominal treatments of simultaneous application of synchronized RF and HIFEM (30 minutes, once per week). Punch biopsies of treated and control subcutaneous tissue were collected at the baseline, 4 days, 2 weeks, 1 month, and 2 months. Specimens were examined by light and scanning electron microscopy. Adipocyte volume was analyzed. Fat tissue temperature was measured in situ (fiber optic probes) and superficially (thermal imager).

RESULTS Fat layer was heated to temperatures of 42 to 45°C. Signs of fat apoptosis (shape alternations and pyknotic nuclei) appeared at day 4 and peaked between 2 weeks and 1 month. Adipocyte volume decreased significantly ($p < .001$) by 31.1% at 2 weeks, 1 month (−23.6%), and 2 months (−22.0%). Control samples showed healthy adipocytes. Scanning electron microscopy micrographs corroborated histology findings, showing flattened, volume-depleted and disrupted adipocytes.

CONCLUSION Synchronized RF with HIFEM procedure resulted in a significant and sustained fat reduction with no adverse events.

Noninvasive techniques for body shaping as an alternative to the invasive methods are generally sought and well accepted by the public because they pose less risk with minimum side effects and no downtime.[1] Novel synchronized radiofrequency (RF) and high-intensity focused electromagnetic (HIFEM) technologies were recently developed to provide noninvasive body shaping using heat and intensive muscle contractions, respectively.

The effect of RF technology is based on generating heat in different tissues through the transformation of RF energy into heat.[2] Certain frequencies of the RF spectrum allow for selective heating of skin or subcutaneous adipose tissue because of the different dielectric properties of biological tissues. Hence, RF is often used for fat removal, skin tightening, or cellulite reduction.[3–8]

High-intensity focused electromagnetic technology induces muscle contractions through stimulation of the nerve pathways. The magnetic field induces electric currents, depolarizing the cell membranes of nerve cells to propagate an action potential and contract muscle fibers.[9] Intense muscle contractions (referred to as supramaximal) result in an increase in the muscle mass through hypertrophy/hyperplasia.[10]

Noninvasive fat reduction requires lipolysis, which is the breakdown of triglycerides stored in the fat cells into glycerol and free fatty acids (FFAs). Radiofrequency-targeted heating of subcutaneous tissue results in increased fat cell metabolism, which facilitates this breakdown.[11,12] In addition, a simultaneous intensive muscle workload, such as during HIFEM treatment, is accompanied by an elevated level of lipolysis due to the increased local energy consumption.[13]

For long-term reduction of subcutaneous fat tissue, necrosis or apoptosis must be achieved and seen on histological studies.[11] Necrosis is immediate cell death that can follow various external factors, such as excessive heat, cold, and toxins, and can lead to untoward side effects.[14,15] It is usually linked with intensive inflammation and possible panniculitis (e.g., significant lymphohistiocytic infiltrate).[16,17] By contrast, apoptosis, a process by which the body replaces old/damaged cells, manifests itself with very mild immune response[18,19] and is therefore known as the

"silent cell death." Importantly, it has been shown that apoptosis is usually a temperature-dependent event. With a minimal 15-minute exposure time, apoptosis can be initiated with temperatures of 42°, and exposure time to trigger apoptosis decreases as the temperature rises. Apoptosis is achieved with temperatures of up to 45°C, whereas higher temperatures may result in immediate cell death or necrosis.[11,20–22] Regarding necrosis versus apoptosis, necrosis is immediate death of tissue that can cause a whole host of problems including panniculitis and should be avoided. Apoptosis is a slow programmed death that is associated with less side effects and is preferable.

When applying RF and HIFEM simultaneously, a primary effect on fat tissue is attributed to the RF-heating–induced apoptosis. Hypothetically, the use of a dual-modality approach might boost the metabolic activity for more effective fat reduction. High-intensity focused electromagnetic contractions might also aid with heat distribution and reduce risk of hot spots.[23,24]

Technical limitations have previously prevented the concurrent use of HIFEM and RF technology because of the interference between 2 competing electromagnetic fields. This study describes a novel synchronized RF that allows simultaneous combination of both technologies. In this porcine study, the use of HIFEM and synchronized RF determines effects on adipose tissue using both H&E histology and scanning electron microscopy (SEM).

Materials and Methods

An institutional review board approved this prospective animal study of 7 large white pigs (females) aged approximately 6 months. The number of animals was chosen to respect the 3Rs principle for animal experimentation as much as possible, and the study was performed in accordance with the EU Directive for animal experiments. A certified veterinarian supervised all the procedures.

All animals received active treatment 1 week after the acclimatization period. Three 30-minute abdominal therapies once a week for 3 weeks per pig were performed using Emsculpt Neo device (BLT Industries Inc., Boston, MA), which simultaneously combines novel synchronized RF and HIFEM technologies in a single applicator. The applicator was placed on the abdominal area, affixed by a fixation belt, and therapy power was set to maximum allowed intensity for both modalities. Animals were under general anesthesia. Before each therapy, anesthetic premedication was performed by the mixture of tiletamine 2 mg/kg, zolazepam 2 mg/kg, ketamine 2 mg/kg, and xylazine 2 mg/kg. During the therapy, anesthesia was maintained because of the continual influx of 2% propofol solution (1–2 mg/kg) by a cannula inserted into the auricular vein. The vital functions of animals were monitored during the therapy.

Using ultrasound guidance (Mindray M5Vet, probe 10L4s), a flexible fiber optic temperature probe (LumaSense Technologies Inc., Raunheim, Hessen, Germany) was inserted into the subcutaneous fat tissue just below the applicator (the middepth of the fat layer) to monitor in situ the temperatures of the adipose tissue during the therapy (Figure 1). The

Figure 1. Fiber optic temperature probe inserted into the mid-depth of subcutaneous tissue. The probe tip (red dot) was located in the center of the shaved treated area (circled). The fiber was fixed by an adhesive tape to prevent its displacement during the therapy.

superficial skin temperature was monitored immediately after removing the applicator at the end of the procedure by a thermal imaging camera (Fluke Ti300, Fluke Corporation).

Biopsy specimens of the fat tissue for histological and SEM examination were collected at baseline, 4 days (D4), 2 weeks (W2), 1 month (M1), and 2 months (M2) posttreatment for each animal by biopsy punch (6 mm in diameter). Two specimens per time point (one for histology and one for SEM) were collected from the treatment site. Control specimens of abdominal fat tissue were collected from the opposite side of each subject animal.

For histological examination, hematoxylin and eosin (H&E) staining was used. In total, 252 tissue slices were analyzed. The samples for SEM were fixed with 3% paraformaldehyde and 2% glutaraldehyde and then gold stained. Micrographs were taken using a JSM-6380LV microscope (Jeol Ltd, Akishima, Japan). Expert evaluation of all slices and micrographs in a random order was performed by an experienced histopathologist.

Adipocyte cross-sectional area measurements were made using ImageJ v1.52p software. The area of fat cells was calculated for each analyzed image. Descriptive statistics (mean and SD) were used to identify the change in adipocyte size. Significance of this change was analyzed by one-way analysis of variance, followed by the Tukey–Kramer post hoc test. A p value less than 0.05 was accepted as the level of statistical significance.

Results

Clinical examination during all phases showed normal health of all animals, and no complications regarding animal care occurred. Animals always recovered well from the anesthesia procedure without any treatment-related complications or side effects.

Temperature Measurements

Subcutaneous fat temperature measured in situ reached 42°C in the first 4 minutes (Figure 2). Then 44°C was reached soon after, and for the rest of the procedure (23 minutes), temperature was maintained in a 44 to 45°C range. The skin temperature measured immediately after the treatment showed safe values between 42°C and 43°C in all animals.
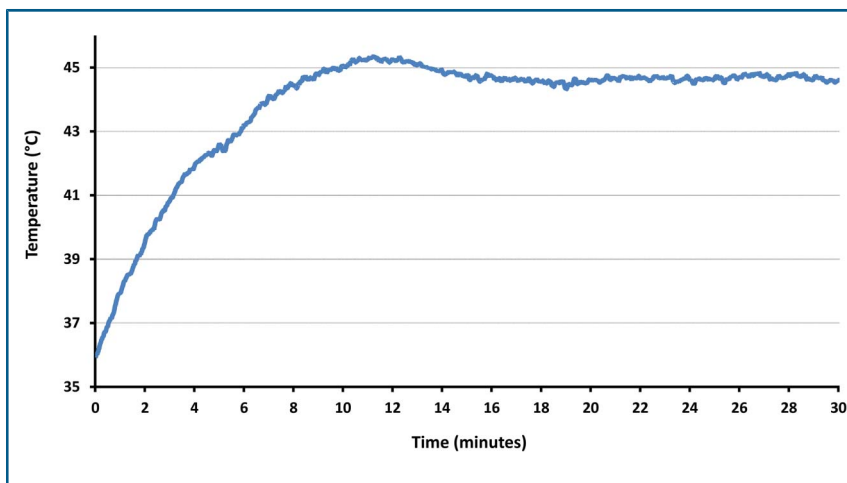
Figure 2. Continuous temperature measurement by the fiber optic probe located in the middle of fat tissue layer depth (Pig No. 3; first therapy, RF, and HIFEM set to maximum allowed intensity). The therapeutic temperature was achieved in the first 4 minutes, and it was maintained at a stable level of 44 to 45°C, during most of the procedure. HIFEM, high-intensity focused electromagnetic; RF, radiofrequency.

Histology Evaluation

Baseline and control samples showed predominantly normal round/polygonal-shaped healthy adipocytes without any damage to fat tissue (Figure 3). Four days after the last treatment, alternations of the cell shape were present. Adipocytes were noticeably flattened and of a smaller size ($p < .001$; Figure 3) with multiple adipose cells showing membrane rupture. Connective tissue (collagen fibers) shows conformational changes. Initiation of a mild inflammatory response was also observed with some neutrophils, lymphocytes, and macrophages seen perivascularly and surrounding adipocytes. The presence of subtle infiltration by these cells indicated that the elimination of damaged fat cells had already been initiated.

Two weeks after the final treatment, adipocytes were flattened and of significantly ($p < .001$) smaller size because of the release of their lipid content caused by the lipolytic effect of the simultaneous application of RF and HIFEM therapy (Figures 3 and 5). Multiple adipocyte nuclei demonstrated pyknotic appearance (a sign of apoptotic changes), as evidenced by their small and shrunk nuclei with dark, highly condensed nuclear chromatin. Furthermore, some membranes manifested rupture with unusual shape alternations, whereas immune cells were observed perivascularly. Macrophages (foamy histiocytes) and lipophages could be seen in areas where the damaged fat cells were being cleared.

One month after the last treatment, unstructured spaces of various sizes were present, caused by the elimination of fat cells (Figure 4). Ruptures in some adipocyte membranes were still visible. The inflammatory infiltrate receded, indicating that the removal of damaged tissue peaked in between 14 and 30 days. The diameter of the intact adipocytes was below the baseline values because they seemed to contain less lipids than pretreatment ($p < .001$; Figure 5).

At 2 months, the inflammatory infiltrate was occasionally present as a part of late tissue healing response along with a few ruptured membranes of adipocytes (Figure 4). Adipocytes showed no major alterations in shape but still remained smaller compared with the baseline ($p < .001$). In addition, as a result of the collagen remodeling induced by the RF,[25] the interlobular septa seemed well-developed. Notably, no damage to the blood vessels or necrosis of the fat tissue was observed.

Area of Adipocytes

Treated adipocytes showed a smaller diameter than at baseline (Figure 5). Overall, the fat tissue showed a
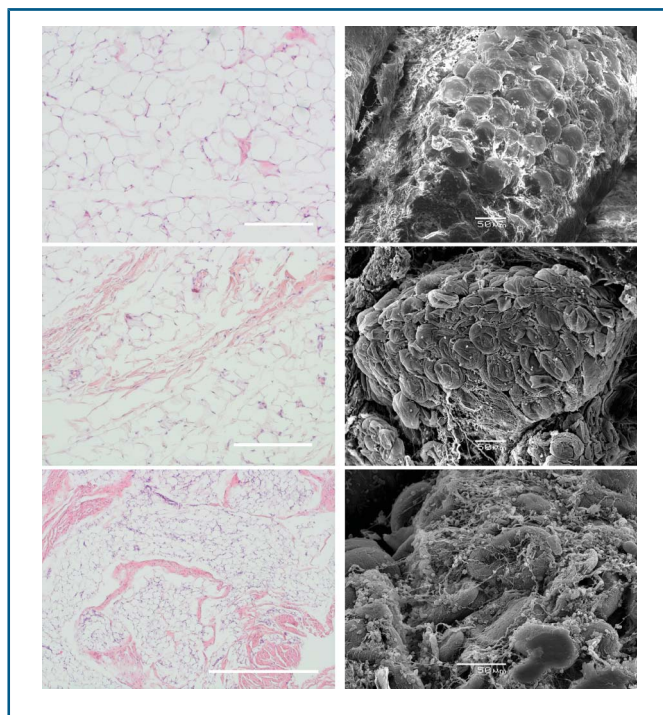

Figure 3. Light microscopy and SEM findings side by side: control/baseline (up, bar = 100 μm), 4 days (mid, bar = 200 μm), and 2 weeks (down, bar = 500 μm). Changes of fat tissue include delaminated membranes of adipocytes, alternations of their shape, presence of pyknotic nuclei, and subtle immune response, which started by day 4 and further propagated at 2 weeks. Conformational changes of collagen fibers were seen by day 4. SEM, scanning electron microscopy.
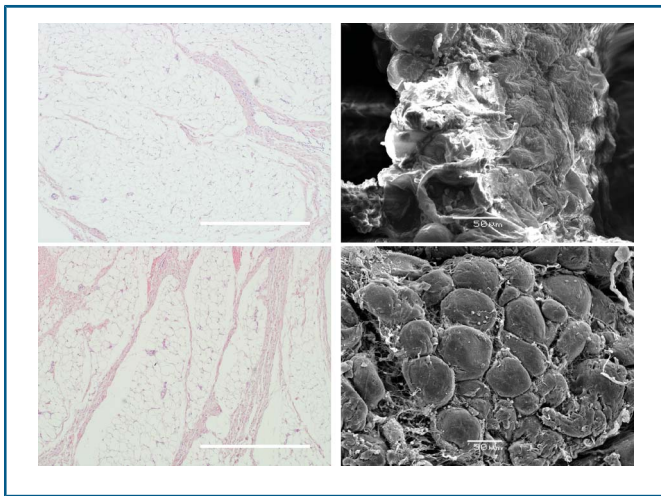
Figure 4. Light microscopy and SEM findings side by side at 1 month (up) and 2 months (down). At 1 month, the adipocytes still show membrane ruptures and alternations of their shape; however, the immune infiltrate is receding. At 2 months, the adipose tissue regenerates and is consisted of healthy-looking fat cells of smaller diameter. The architecture of interlobular septa was noticeably improved. SEM, scanning electron microscopy.

considerable decrease of adipocytes' area with the greatest reduction observed at 4 days (-25.9%; $-337.8\ \mu m^2$) and 2 weeks (-31.1%; $-405.5\ \mu m^2$) after the last procedure, when the most prominent changes in fat tissue were observed. Notably, the size of the adipocytes remained smaller at 1-month and 2-month follow-up compared with the baseline.

Scanning Electron Microscopy

Scanning electron microscopy micrographs corroborate the histology findings (Figures 3 and 4). At baseline, once again, healthy fat cells with well-defined shapes were observed. At the same time, 4 days after the last treatment, the adipocytes shrunk by 30% because of lipolysis with noticeable signs of membrane rupture. Fat cell elimination was more pronounced at 2 weeks with clearly visible lipolysis and the

apoptotic events (Figure 3). A large number of disrupted adipocytes with extrusion of lipid droplets outside the ruptured and damaged cells were observed. A mild inflammatory infiltrate was present, indicating a local response to remove adipocyte cell remains.[20,21]

At 1 month, SEM micrographs showed that the adipose tissue still contained some damaged adipocytes, which had not yet been cleared (Figure 4). Surviving adipocytes were smaller because of lipolysis but showed signs of recovery and restoration of cell shape. Finally, 2 months after treatments, volume-depleted surviving adipocytes were almost back to baseline, although they still occasionally showed shape alternations (Figure 4).

Discussion

The histological and SEM evaluation of fat tissue after the dual RF/HIFEM treatment showed a corresponding pattern. Both H&E and SEM demonstrated lipolysis and a decrease in fat cells predicted to be long-term. Treatment effects in fat tissue peaked between 2 weeks and 1-month posttreatment when the most significant changes were seen. At 2 months, fat tissue still showed a significant and sustained fat reduction.

To accomplish a therapeutic effect in adipose tissue, it is necessary to achieve heating in a narrow range of 42 to 45°C, which triggers alternations in the structural integrity of the fat cells.[2,15] As shown in Figure 2, the lower limit of this temperature range was already achieved during the first 4 minutes. Temperature was then maintained within this range for the rest of the treatment. Such a rapid increase followed by a steady temperature profile allows for high efficiency because the therapeutic effect is delivered for 26 minutes of 30. This temperature profile is believed to be attributed to more uniform distribution of RF-generated heat, which is augmented by concomitant muscle activity and augmented blood circulation.[24] This hypothetically eliminates hot spots and contributes to treatment efficacy.

Previous studies have shown that controlled RF heating used as a standalone modality induces apoptosis.[20,21] Because only a mild inflammation response was observed, we believe
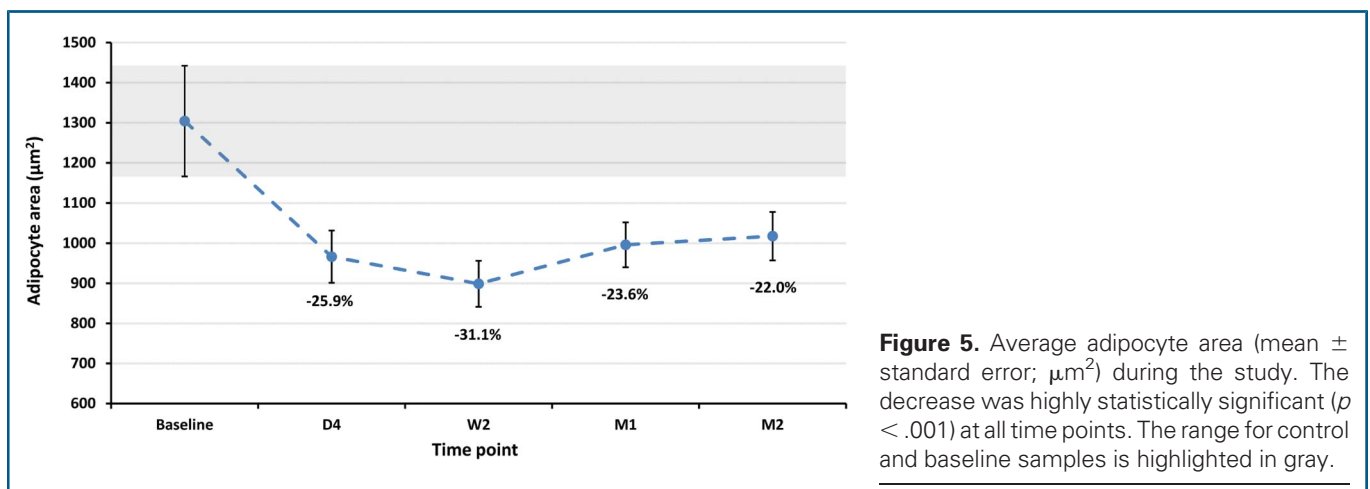

Figure 5. Average adipocyte area (mean ± standard error; μm^2) during the study. The decrease was highly statistically significant ($p < .001$) at all time points. The range for control and baseline samples is highlighted in gray.

that heat-induced necrosis was not the primary effect. This study shows that apoptosis is the more predominant mechanism than necrosis, with treated adipocytes showing pyknotic nuclei, delaminated membranes, shape alternations, and only a mild inflammatory response. Adipocytes also suffer apoptosis when their size significantly fluctuates while becoming too large or too small[11,26] and are stressed by the excessive efflux of FFAs.[13,27] Although RF is assumed to play a major role in the effect on fat tissue, HIFEM-induced lipolysis may augment the overall fat cell shrinkage and thus enhance the apoptotic effect of the RF treatment.

We believe that the very significant lipolysis observed in this study reflects simultaneous use of both modalities. First, RF heats the tissue and activates the sympathetic branch of the autonomic nervous system. This leads to the release of catecholamines (adrenaline and noradrenaline), which triggers lipolysis.[5] The magnetic field simultaneously applied leads to intense muscle contractions that requires considerable amount of energy. This additional energy demand is believed to stress adipocytes to deliver more by increasing metabolic pathways such as breakdown of triglycerides. More triglycerides are broken to FFAs, which are delivered through the circulation to the muscle tissue for β-oxidation and ATP production.[28]

Although RF heating alone induces lipolysis, some of the released FFAs may be a subject to lipogenesis if not consumed for energy, which may occur in all noninvasive fat reduction modalities.[26] The results from our study showed a sustained reduction of fat cells' size after 2 months, indicating that lipolysis was predominant. A major role in long-term fat reduction is extensive apoptosis. Our study shows extensive fat cell disruption by apoptosis in histological and SEM images.

In safety, neither RF (when used within safe parameters) nor HIFEM injures the skin, blood vessels, or other adjacent structures when used as a standalone modality for non-invasive body shaping.[3,5,8,11,13,20,23,27,29] This porcine study corroborates this finding with additional effects of better organization of interlobular septa with RF-induced activation of fibroblasts and subsequent collagen remodeling.[25,30] This study objectively shows effects of novel simultaneous synchronized RF and HIFEM technologies for porcine subcutaneous fat reduction. Limitations include whether this animal study will reflect results in human, although previous studies have shown that results in porcine models often reflect the results in human fat tissue.[31,32]

Conclusion

Simultaneous delivery of synchronized RF and high-intensity focused electromagnetic procedure demonstrated an excellent safety profile with no adverse events documented after 3 weekly treatments in a porcine model. Histology and SEM examination of adipose tissue revealed strong evidence of elimination of adipocytes through an apoptotic mechanism accompanied by a lipolytic effect, resulting in an overall fat tissue reduction. Induced changes were observed to peak during the first month, whereas at 2 months, a significant reduction of fat tissue was observed.

References

1. The American Society for Aesthetic Plastic Surgery. 2018 procedural statistics. Available from: https://www.surgery.org/media/statistics. Accessed January 2020.
2. Goats GC. Continuous short-wave (radio-frequency) diathermy. *Br J Sports Med* 1989;23:123–7.
3. Trelles MA, van der Lugt C, Mordon S, Ribé A, et al. Histological findings in adipocytes when cellulite is treated with a variable-emission radiofrequency system. *Lasers Med Sci* 2010;25:191–5.
4. Tanaka Y, Tsunemi Y, Kawashima M, Tatewaki N, et al. Treatment of skin laxity using multisource, phase-controlled radiofrequency in asians: visualized 3-dimensional skin tightening results and increase in elastin density shown through histologic investigation. *Dermatol Surg* 2014;40:756–62.
5. Vale AL, Pereira AS, Morais A, Noites A, et al. Effects of radio-frequency on adipose tissue: a systematic review with meta-analysis. *J Cosmet Dermatol* 2018;17:703–11.
6. Emilia del Pino M, Rosado RH, Azuela A, Graciela Guzmán M, et al. Effect of controlled volumetric tissue heating with radiofrequency on cellulite and the subcutaneous tissue of the buttocks and thighs. *J Drugs Dermatol* 2006;5:714–22.
7. Trelles MA, Mordon SR. Adipocyte membrane lysis observed after cellulite treatment is performed with radiofrequency. *Aesthet Plast Surg* 2009;33:125–8.
8. Weiss RA. Noninvasive radio frequency for skin tightening and body contouring. *Semin Cutan Med Surg* 2013;32:9–17.
9. Roth BJ, Basser PJ. A model of the stimulation of a nerve fiber by electromagnetic induction. *IEEE Trans Biomed Eng* 1990;37:588–97.
10. Duncan D, Dinev I. Noninvasive induction of muscle fiber hypertrophy and hyperplasia: effects of high-intensity focused electromagnetic field evaluated in an in-vivo porcine model: a pilot study. *Aesthet Surg J* 2020;40:568–74.
11. Duncan DI, Kim THM, Temaat R. A prospective study analyzing the application of radiofrequency energy and high-voltage, ultrashort pulse duration electrical fields on the quantitative reduction of adipose tissue. *J Cosmet Laser Ther* 2016;18:257–67.
12. Kinney BM, Kanakov D, Yonkova P. Histological examination of skin tissue in the porcine animal model after simultaneous and consecutive application of monopolar radiofrequency and targeted pressure energy. *J Cosmet Dermatol* 2020;19:93–101.
13. Halaas Y, Bernardy J. Mechanism of nonthermal induction of apoptosis by high-intensity focused electromagnetic procedure: biochemical investigation in a porcine model. *J Cosmet Dermatol* 2020;19:605–11.
14. Levi JR, Veerappan A, Chen B, Mirkov M, et al. Histologic evaluation of laser lipolysis comparing continuous wave vs pulsed lasers in an in vivo pig model. *Arch Facial Plast Surg* 2011;13:41–50.
15. Decorato JW, Chen B, Sierra R. Subcutaneous adipose tissue response to a non-invasive hyperthermic treatment using a 1,060 nm laser. *Lasers Surg Med* 2017;49:480–9.
16. Preciado JA, Allison JW. 59. The effect of cold exposure on adipocytes: examining a novel method for the non-invasive removal of fat. *Cryobiology* 2008;57:327.
17. Manstein D, Laubach H, Watanabe K, Farinelli W, et al. Selective cryolysis: a novel method of non-invasive fat removal. *Lasers Surg Med* 2008;40:595–604.
18. Chen GY, Nuñez G. Sterile inflammation: sensing and reacting to damage. *Nat Rev Immunol* 2010;10:826–37.
19. Rock KL, Kono H. The inflammatory response to cell death. *Annu Rev Pathol Mech Dis* 2008;3:99–126.
20. Boisnic S, Divaris M, Nelson AA, Gharavi NM, et al. A clinical and biological evaluation of a novel, noninvasive radiofrequency device for the long-term reduction of adipose tissue. *Lasers Surg Med* 2014;46:94–103.
21. McDaniel D, Fritz K, Machovcova A, Bernardy J. A focused monopolar radiofrequency causes apoptosis. *A Porcine Model* 2014;13:5.
22. Fenn AJ. *Breast Cancer Treatment by Focused Microwave Thermotherapy*. Oxfordshire, United Kingdom: Taylor & Francis, Jones & Bartlett Learning; 2007.

23. Adatto MA, Adatto-Neilson RM, Morren G. Reduction in adipose tissue volume using a new high-power radiofrequency technology combined with infrared light and mechanical manipulation for body contouring. *Lasers Med Sci* 2014;29:1627–31.

24. Joyner MJ, Casey DP. Regulation of increased blood flow (hyperemia) to muscles during exercise: a hierarchy of competing physiological needs. *Physiol Rev* 2015;95:549–601.

25. Meyer PF, de Oliveira P, Silva FKBA, da Costa ACS, et al. Radio-frequency treatment induces fibroblast growth factor 2 expression and subsequently promotes neocollagenesis and neoangiogenesis in the skin tissue. *Lasers Med Sci* 2017;32:1727–36.

26. Jo J, Shreif Z, Periwal V. Quantitative dynamics of adipose cells. *Adipocyte* 2012;1:80–8.

27. Weiss RA, Bernardy J. Induction of fat apoptosis by a non-thermal device: mechanism of action of non-invasive high-intensity electromagnetic technology in a porcine model. *Lasers Surg Med* 2019;51:47–53.

28. Lass A, Zimmermann R, Oberer M, Zechner R. Lipolysis—a highly regulated multi-enzyme complex mediates the catabolism of cellular fat stores. *Prog Lipid Res* 2011;50:14–27.

29. Pumprla J, Howorka K, Kolackova Z, Sovova E. Non-contact radiofrequency-induced reduction of subcutaneous abdominal fat correlates with initial cardiovascular autonomic balance and fat tissue hormones: safety analysis. *F1000Research* 2015;4:49.

30. Yokoyama Y, Akita H, Hasegawa S, Negishi K, et al. Histologic study of collagen and stem cells after radiofrequency treatment for aging skin. *Dermatol Surg* 2014;40:390–7.

31. Wang Q, Wang J, Wang T. Pigs can Be used as a large animal model for autologous fat grafting. *Ophthal Plast Reconstr Surg* 2016;32:73–4.

32. Houpt KA, Houpt TR, Pond WG. The pig as a model for the study of obesity and of control of food intake: a review. *Yale J Biol Med* 1979;52:307–29.